Section 3 Auditory Physiology

Chapter 1. Signal Transmission in the Auditory System

Academic and Research Staff

Professor Dennis M. Freeman, Professor Lawrence S. Frishkopf, Professor Nelson Y.S. Kiang, Professor William T. Peake, Professor William M. Siebert, Professor Thomas F. Weiss, Dr. Peter Cariani, Dr. Bertrand Delgutte, Dr. Donald K. Eddington, Dr. John J. Guinan, Jr., Dr. William M. Rabinowitz, Dr. Christopher A. Shera, Marc A. Zissman

Visiting Scientists and Research Affiliates

Dr. Robert D. Hall, Dr. Ruth Y. Litovsky, Dr. Sunil Puria, Michael E. Ravicz, Dr. John J. Rosowski, Joseph Tierney

Graduate Students

C. Cameron Abnet, Alexander J. Aranyosi, C. Quentin Davis, Scott B.C. Dynes, Benjamin M. Hammond, Shilpa M. Hattangadi, Gregory T. Huang, John R. Iversen, Laura K. Johnson, Sridhar Kalluri, Zoher Z. Karu, Christopher J. Long, Martin F. McKinney, Pankaj Oberoi, Mark N. Oster, Lisa F. Shatz, Janet L. Slifka, Konstantina M. Stankovic, Thomas M. Talavage, Su W. Teoh, Susan E. Voss

Undergraduate Students

Arash Lighvani, Christopher McKinney, Rosanne Rouf

Technical and Support Staff

Janice L. Balzer, David A. Steffens

1.1 Introduction

Research on the auditory system is carried out in cooperation with two laboratories at the Massachusetts Eye and Ear Infirmary (MEEI). Investigations of signal transmission in the auditory system involve the Eaton-Peabody Laboratory for Auditory Physiology. The Eaton-Peabody Laboratory's long-term objective is to determine the anatomical structures and physiological mechanisms that underlie vertebrate hearing and apply this knowledge to clinical problems. Studies of cochlear implants in humans are carried out at the MEEI Cochlear Implant Research Laboratory. Cochlear implants electrically stimulate intracochlear electrodes to elicit patterns of auditory nerve fiber activity that the brain can learn to interpret. The ultimate goal for these devices is to provide speech communication for the profoundly deaf.

1.2 Middle and External Ear

Sponsors

National Institutes of Health
Grant P01-DC-00119
Grant R01-DC-00194

Project Staff

Professor John J. Rosowski, Professor William T. Peake, Dr. Sunil Puria, Greg T. Huang, Michael E. Ravicz, Su W. Teoh, Susan E. Voss

1.2.1 Overall Goal

Our aim is to determine how the structure of the normal and pathological external and middle ear effects their acoustic and mechanical functions. To achieve this aim, we investigate the functions of the varied ear structures found in animals as well as measuring the function of normal and pathologic human middle ears. Acoustic and mechanical measurements are used to generate testable quantitative models of external and middle-ear function.

1.2.2 Middle-Ear Structure and Function

Last year, our studies of the structure and function of the middle-ears of different animals followed four paths: (1) tests of the common assumption that the cochlea responds to the difference in sound pressure at the two cochlear windows; (2) measurement of the acoustic function of an anatomically distinct section of the tympanic membrane, the *pars flaccida*; (3) an analysis of acoustic power flow through the external and middle ear in gerbils; and (4) a study of how the size of the ear effects middle-ear function. The first study confirmed that the window pressure difference is the primary cochlear input.[1] The second study resulted in the first demonstration of a role for *pars flaccida* in limiting the low-frequency response of the middle ear.[2] The third study, described in a paper which is forthcoming, demonstrated that the power-collection performance of the gerbil external and middle plays a large role in determining the overall shape of the gerbil audiogram. The fourth study compared middle-ear function in ears of similar structure, but greatly different size; the ears of house cats were compared with those of a lion. This work led to a quantitative rule relating skull length and middle-ear cavity function that was the subject of a meeting presentation.

Basic and Clinical Studies of the Human Middle Ear

Our work on human middle-ear function revolved around model analyses of surgical procedures used to reconstruct diseased middle ears. These studies led to three publications that presented surgical rules that could be used to improve the acoustic and mechanical function of diseased middle ears.

1.2.3 Publications

Journal Articles

Merchant S.N., J.J. Rosowski, and M.E. Ravicz. "Mechanics of Type IV and V Tympanoplasty. II. Clinical Analysis and Surgical Implications." *Am. J. Otol.* 16: 565-575 (1995).

Ravicz M.E., J.J. Rosowski, and H.F. Voigt. "Sound-power Collection by the Auditory Periphery of the Mongolian Gerbil Meriones unguiculatus: II. External-ear Radiation Impedance and Power Collection." *J. Acoust. Soc. Am.* Forthcoming.

Rosowski J.J. and S.N. Merchant. "Mechanical and Acoustical Analyses of Middle-ear Reconstruction." *Am. J. Otol.* 16: 486-497 (1995).

Rosowski J.J., S.N. Merchant, and M.E. Ravicz. "Mechanics of Type IV and V Tympanoplasty. I. Model Analysis and Predictions." *Am. J. Otol.* 16: 555-564 (1995).

Voss S.E., J.J. Rosowski, and W.T. Peake. "Is the Pressure Difference Between the Oval and Round Windows the Effective Acoustic Stimulus for the Cochlea?" Submitted to *J. Acoust. Soc. Am.*

Meeting Paper

Rosowski J.J., W.T. Peake, G.T. Huang, and D.T. Flandermeyer. "Middle-ear Structure and Function in the Family *Felidae*." *Abstracts of the Eighteenth Midwinter Meeting of the Association for Research in Otolaryngology,* St. Petersburg, Florida, February 5-9, 1995, p. 5.

Theses

Teoh, S.W. *The Pars flaccida of the Gerbil Middle Ear.* S.M. thesis. Dept. of Electr. Eng. and Comput. Sci., MIT, 1995.

Voss, S.E. The *Cochlear Windows of the Cat.* S.M. thesis. Dept. of Electr. Eng. and Comput. Sci., MIT, 1995.

1.2.4 Cochlear Mechanisms

Sponsor

National Institutes of Health
Grant R01 DC00238

Project Staff

Professor Thomas F. Weiss, Professor Dennis M. Freeman, C. Cameron Abnet, Alexander J. Aranyosi, C. Quentin Davis, Shilpa M. Hattangadi, Laura K. Johnson, Zoher Z. Karu, Rosanne Rouf, Lisa F. Shatz, Janet L. Slifka

---

[1] S.E. Voss, *The Cochlear Windows of the Cat,* S.M. thesis, Dept. of Electr. Eng. and Comput. Sci., MIT, 1995.

[2] S.W. Teoh, *The Pars flaccida of the Gerbil Middle Ear,* S.M. thesis, Dept. of Electr. Eng. and Comput. Sci., MIT, 1995.

1.2.5 Using Video Microscopy to Measure Microscopic Motions

We have developed a video system to measure sound-induced motions of cochlear structures in the inner ear. The system uses a light microscope to project magnified images of cochlear structures onto a scientific grade CCD camera. Images from a series of focal depths are combined into a three-dimensional image that characterizes all of the structures in the cochlea including the basilar membrane, tectorial membrane, and sensory receptor (hair) cells. Stroboscopic illumination is used to obtain a sequence of three-dimensional images that are phase-locked to the audio-frequency hydrodynamic stimulus.

Development of Motion Detection Algorithms

Even after magnification by a light microscope, sound-induced motions of cochlear structures are smaller than the pixel spacing of a modern CCD camera. We have investigated two broad classes of algorithms for estimating subpixel displacements. The first class is based on optical flow and exploits relations between temporal and spatial derivatives of image brightness to estimate displacement. The second class is block-matching and determines translations between images by minimizing the difference between shifted versions of the original images. These two classes of algorithms were thought to be completely different, and the accuracy of subpixel estimates based on algorithms from the two classes have been reported to differ.[3] However, we have proven that if you choose corresponding algorithms from the two classes, the estimators are identical.[4] This insight has important consequences. Many properties of motion estimates are more easily understood when cast as an optical flow formulation; others are more easily understood when cast as block-matching. Furthermore, the computational costs for the two formulations are different. Knowing that the classes are equivalent allows one to capitalize on the strengths of each formulation.

Measurement of Sound-Induced Motion of Cochlear Structures

To characterize the relation between motion of a hair bundle and the overlying tectorial membrane, we analyzed motions of the structures in six planes of focus separated by 3 μm.[5] Displacements near the base of the hair bundle were larger than those near the tip (figure 1), which demonstrates that the hair bundle is rotating about its point of attachment to the hair cell. Displacements of the tectorial membrane were generally smaller than those of either the base or tip of the hair bundle. Furthermore, as distance from the base of the hair bundle increases, the motion shows increasing phase lag. In our 12 experiments to date, displacements of the tips and bases of hair bundles have been larger than those of the overlying tectorial membrane for frequencies throughout the lizard's auditory range. This result is consistent with the idea that inertial forces arising from the mass of the tectorial membrane and surrounding fluid tend to resist motion of the tectorial membrane.[6] This result is not consistent with other theories that suggest that the tectorial membrane is a resonant structure.[7] However, our results should be regarded as preliminary. Control experiments must be performed to assure that the cochlea is not damaged during experimentation.

The same data set used in the previous analysis can also be used to study mechanical events at the level of individual sensory hairs. The sinusoidal stimulus generates nearly sinusoidal motions of all the sensory hairs (top right panel of figure 2). To determine if there is relative motion between the sensory hairs, we applied our motion detection algorithm to estimate the motion of the right edge of the bundle and shifted the images to compensate for that motion. The resulting images show relative motions between sensory hairs (bottom right panel of figure 2). Motions of individual sensory hairs have been measured elsewhere,[8] but only for hair

---

3 Q. Tian and M.N. Huhns, "Algorithms for Subpixel Registration," *Comput. Vision, Graphics Image Proc.* 35: 220-233 (1986).

4 C.Q. Davis, Z.Z. Karu, and D.M. Freeman, "Equivalence of Block Matching and Optical Flow Based Methods of Estimating Sub-pixel Displacements," *IEEE International Symposium for Computer Vision,* 1995, pp. 7-12.

5 D.M. Freeman and C.Q. Davis, "Using Video Microscopy to Characterize Micromechanics of Biological and Man-made Micromachines," Solid-State Sensor and Actuator Workshop, Hilton Head Island, South Carolina, June 2-6, 1996, forthcoming.

6 F. Mammano and R. Nobili, "Biophysics of the Cochlea: Linear Approximation," *J. Acoust. Soc. Am.* 93: 3320-3332 (1993).

7 J.B. Allen, "Cochlear Micromechanics: A Physical Model of Transduction," *J. Acoust. Soc. Am.* 68: 1660-1670 (1980).

8 R.K. Duncan, H.N. Hernandez, and J.C. Saunders, "Relative Stereocilia Motion of Chick Cochlear Hair Cells during High-frequency Water-jet Stimulation." *Aud. Neurosci.* 1: 321-329 (1995); R.B. MacDonald and D.P. Corey, "Stereocilia Bundles of the Bullfrog

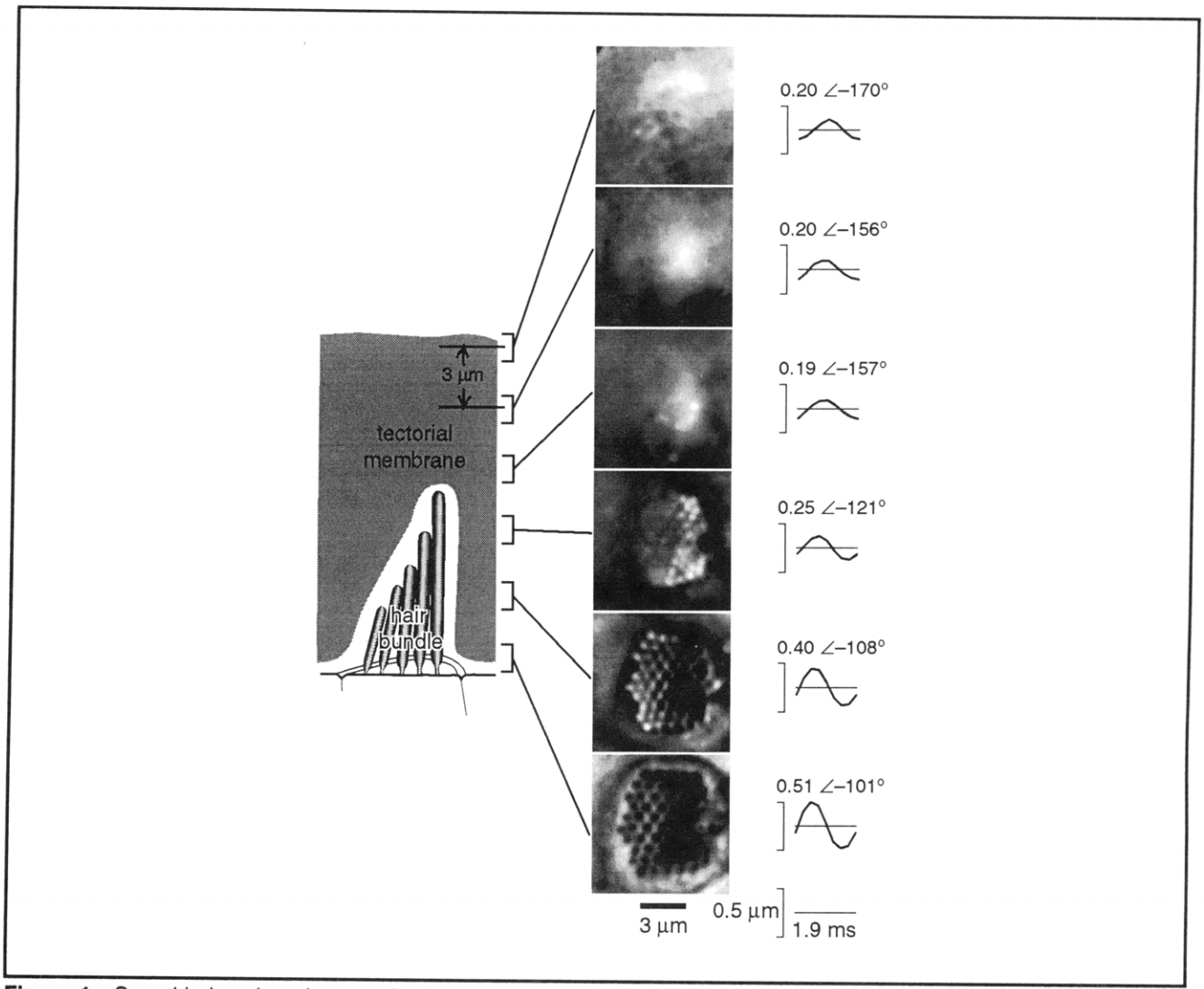

Figure 1. Sound-induced motions at six planes of focus through a hair bundle and overlying tectorial membrane. The intensity of the 513 Hz stimulus (115 dB SPL in the fluid adjacent to the basilar membrane) corresponds to approximately 89 dB SPL at the tympanic membrane. The left panel is a drawing of the hair bundle and overlying tectorial membrane. The center panels are images taken with our measurement system. Similar images acquired at eight different phases of the stimulus period were analyzed to quantify motion at the plane of each section. The waveforms (right panels) are the average horizontal displacements during one period of the stimulus. The numbers above each waveform give the peak-to-peak magnitude (in μm) and angle (in degrees) of the fundamental component of the displacement.

bundles that were stimulated with a water jet; the membranes through which natural stimuli are delivered had been removed.

Application of the Video System to Measure Man-Made Micromachines

Although originally developed to measure motions of cochlear structures, our video system has broader applications. Figure 3 shows results obtained for a man-made micromachine—a folded-

Sacculus Hair Cells Do Not Splay in Response to Stimulation." *Abstracts of the Nineteenth Midwinter Research Meeting of the Association for Research in Otolaryngology,* St. Petersburg, Florida, February 4-8, 1996.

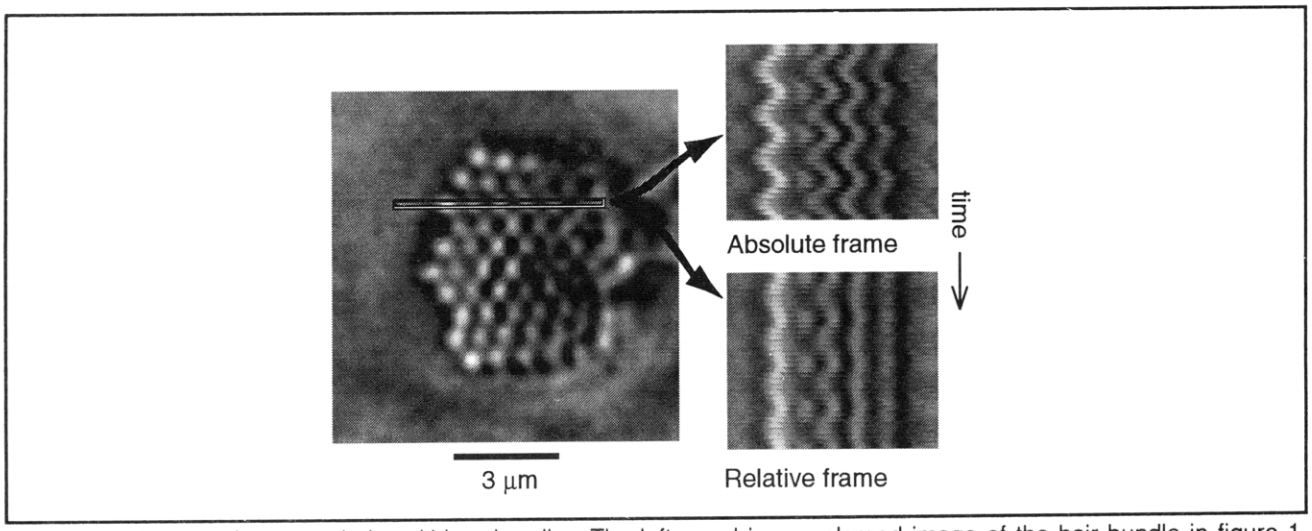

Figure 2. Motions of sensory hairs within a bundle. The left panel is an enlarged image of the hair bundle in figure 1, at a plane of section near the center of the bundle. The highlighted region was extracted from each of eight images acquired during eight evenly spaced phases of the stimulus period. The resulting regions were stacked one on top the next and repeated four times to generate the images in the right panels. The upper and lower right panels are similar, except that the images used to generate the lower panel were first shifted to cancel the motion of the right part of the hair bundle.

beam cantilever.[9] This is a silicon structure that was fabricated by surface micromachining techniques. Using our measurement system, we measured motions of the shuttle in the horizontal direction and also in orthogonal directions. The motions in orthogonal directions represent failure modes for the device—failure modes that our motion measurement system can characterize. Characterizing failure modes can serve two important functions. First, it can help design engineers characterize and avoid failure modes. Second, the system may enable device fabricators to determine whether devices function properly before they are packaged. Such a system could even enable fabricators to correct minor problems using techniques such as laser trimming.

1.2.6 Material Properties of the Tectorial Membrane

Based on its biochemical composition and ultrastructure, the tectorial membrane (TM) is a polyelectrolyte gel. Such gels consist of macromolecules with ionizable fixed charges, small solutes (including ions), and water. Many of the physicochemical properties of polyelectrolyte gels depend on the fixed charge concentration. For example, if the magnitude of the fixed charge concentration increases, mobile counterions will be drawn into the gel to maintain bulk electroneutrality. The increased concentration of mobile counterions represents an increase in osmotic pressure in the gel. Therefore water will flow into the gel and the gel will swell.

Knowledge about the pH dependence of charge groups in TM macromolecules can be used to test the importance of fixed charge in determining the material properties of the TM. If fixed charge density plays an important role, then changes in pH should result in predictable changes in TM volume. We have measured changes in the size and shape of the isolated TM of the mouse to changes in the pH of the surrounding bath.[10] Altering the pH from 7 to a value between 5 and 11 caused changes of both the thickness and volume of the TM that were highly correlated; there was little change in surface area. Changes in thickness for pH between 6 and 9 were small: on the order of 1 percent. In basic solutions, swelling increased with pH: from <1 percent at pH 9 to 9 percent at pH 10 to 79 percent at pH 11. In mildly acidic solutions, thickness

---

9 D.M. Freeman and C.Q. Davis, "Using Video Microscopy to Characterize Micromechanics of Biological and Man-made Micromachines," Solid-State Sensor and Actuator Workshop, Hilton Head Island, South Carolina, June 2-6, 1996, forthcoming.

10 D.M. Freeman, S.M. Hattangadi, and T.F. Weiss, "Osmotic Responses of the Isolated Mouse Tectorial Membrane to Changes in pH," *Abstracts of the Nineteenth Midwinter Research Meeting of the Association for Research in Otolaryngology,* St. Petersburg, Florida, February 4-8, 1996.

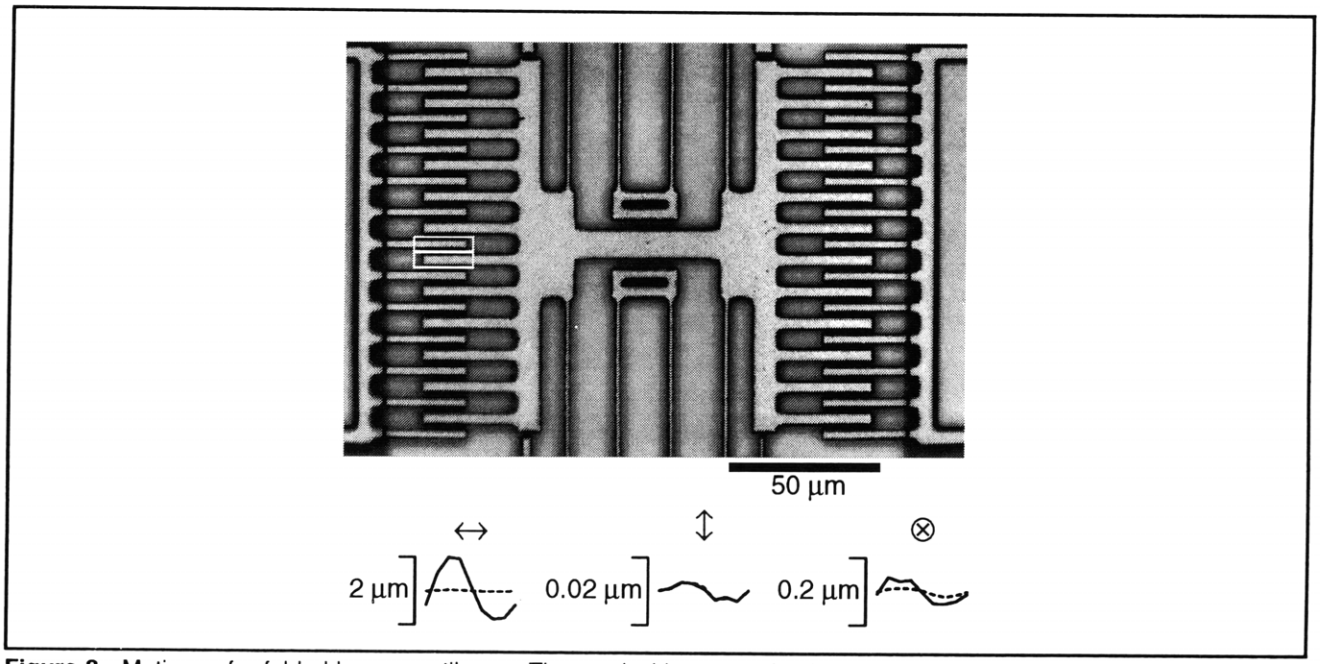

Figure 3. Motions of a folded-beam cantilever. The comb drive was stimulated with a 10 Hz sinusoidal voltage, 44 volts peak-to-peak with an 80 volt DC offset. Images such as the one shown here were obtained at 45 planes of focus with 0.45 μm spacing to generate a three-dimensional image. Three-dimensional images were obtained at eight equally-spaced phases during the stimulus period. The portions of the images in the white boxes were analyzed to determine the motions of a stationary (top) and moving (bottom) tooth of the comb drive, shown in the three plots as dashed and solid curves, respectively. Displacements of the moving tooth were approximately 2 μm peak-to-peak in the horizontal direction (left plot, solid line). Vertical motions (center plot, solid line) were about 5 nm peak-to-peak, which is near the noise floor of our measurement system (without averaging). Motions orthogonal to the plane of focus were 0.08 μm peak-to-peak for the moving tooth (right plot, solid line). Motions of the stationary tooth (dashed lines), which serve as control measurements to assess the stability of the measurement system, were 47, 6, and 26 nm peak-to-peak in the horizontal, vertical, and out of the plane directions, respectively.

decreased to a local minimum of -1 percent near pH 6 which suggests that this is an isoelectric point of the TM. Thickness swelled in more acidic solutions, reaching a local maximum of 14 percent near pH 5.25. In solutions with very low pH (<4), the radial dimension and area of the TM decreased rapidly and monotonically while the thickness of the TM increased transiently and then decreased.

We have also measured osmotic responses of the mouse TM to isosmotic changes in the concentrations of sodium, potassium, and calcium in the bath.[11] Substitution of sodium for potassium as the predominant cation in the bath caused the TM to swell by an amount that depended on calcium concentration. Swelling was about 1 percent when the calcium concentration was 20 μmol/L (similar to that of endolymph), 14 percent when the calcium concentration was less than 7 μmol/L, and less than 1 percent when the calcium concentration was 2 mmol/L. Increasing calcium concentration without changing the predominant cation caused the TM to shrink. Decreasing calcium concentration by removal of calcium or by the addition of the calcium chelator EGTA caused the TM to swell.

To provide a conceptual framework for our measurements and to guide further experimental studies, we have analyzed the equilibrium behavior of an isotropic polyelectrolyte gel model of the TM.[12] The theory presumes that: (1) the gel is homogeneous and isotropic; (2) all ions in the gel are in electrodiffusive equilibrium with the bath ions; (3) the total charge density in the gel is zero; (4) the gel is in osmotic equilibrium with the bath; (5) the hydrodynamic pressure in the gel is proportional to

[11] D.M. Shah, D.M. Freeman, and T.F. Weiss, "The Osmotic Response of the Isolated, Unfixed Mouse Tectorial Membrane to Isosmotic Solutions: Effect of Na^+, K^+, and Ca^{2+} Concentration," *Hear. Res.* 87: 187-207 (1995).

[12] T.F. Weiss and D.M. Freeman, "Isotropic Polyelectrolyte Gel Model of the Tectorial Membrane," *Abstracts of the Nineteenth Midwinter Research Meeting of the Association for Research in Otolaryngology,* St. Petersburg, Florida, February 4-8, 1996.

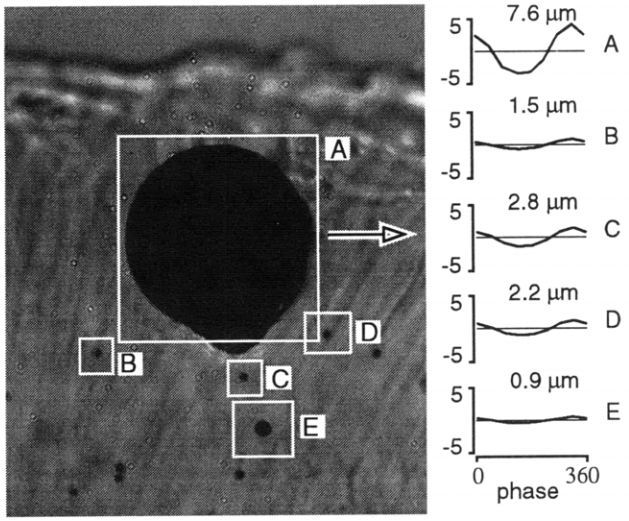

Figure 4. Image of an isolated mouse TM with a 50 μm iron bead (region A) fixed to its surface. A force of 10 μN at 10 Hz is applied to the bead using electromagnets. The magnitudes of deformations for the five highlighted regions are plotted versus the phase of the force excitation. Positive deformations are in the direction of the arrow. The number above each plot indicates the peak-to-peak amplitude of deformation.

the volume increment; and (6) fixed charge groups in the gel are in chemical equilibrium with the mobile ions. Results demonstrate important properties of gels—including their ability to concentrate ions, generate an electrical potential, and swell. The model demonstrates how these properties are linked to the concentration of fixed charge in the gel. The model also allows us to predict the fixed charge concentration of the TM using previously published[13] measurements of the electrical potential of the TM in solutions with different osmolarities. The resulting estimate is within a factor of three of estimates based on biochemical analyses.

1.2.7 Mechanical Properties of the Tectorial Membrane

We have developed a new method for applying calibrated forces to microscopic tissue samples. The forces generate deformation of the tissue that can be measured with video microscopy. The system has been applied to the investigation of the material properties of the TM, which are thought to play a key role in hearing.

The tectorial membrane of a mouse is isolated from the tissue that normally surrounds it and attached to a glass slide. A small iron bead is then fixed to the surface of the tissue. An external magnetic field generates forces on the bead that are transmitted to the TM. The forces, parallel to the tissue surface, generate deformations of the tissue that provide information about its mechanical properties. Forces can be applied to different regions, in different directions, and at various frequencies to obtain information about the tissue's mechanical properties.

Figure 4 illustrates a typical result in which a 10 μN force caused a 7.6 μm displacement of the iron bead. This result indicates that the portion of the TM attached to the bead had an effective stiffness of 1.3 N/m. Parts of the TM near the iron bead also move, but the displacements decrease with distance from the bead with a space constant of approximately 10 μm. Both the space constant and effective stiffness are determined by (1) the material properties of the TM, (2) the geometry of the TM, and (3) the attachment of the TM to the glass slide. We are currently developing a mechanical model to quantify the importance of each of these factors. Results are important for understanding the role that the TM plays in determining the motions of hair bundles.

[13] K.P. Steel, "Donnan Equilibrium in the Tectorial Membrane," *Hear. Res.* 55: 263-272 (1983).

1.2.8 Regulation of pH by Cochlear Hair Cells

As part of a project to quantify the mechanisms that regulate intracellular ion concentrations of hair cells, we are studying the regulation of hair cell pH. Since hair cells carry auditory information in the form of ionic signals, maintenance of the cells' ion concentrations is vital to their function in hearing. Maintenance of pH in particular is important for the function of many cellular enzymes, and it has recently been suggested that acoustic stimulation can affect hair cell pH.[14]

Hair cells in an in vitro preparation of the cochlea of the alligator lizard are loaded with the fluorescent dye BCECF, whose fluorescence intensity is a function of pH. Changes in dye fluorescence are measured using a video microscope and calibrated to estimate pH. Figure 5 illustrates results of an experiment in which 20 mM proprionic acid is transiently added to the artificial perilymph bathing the cochlea. Because proprionic acid permeates membranes quickly, the intracellular pH of hair cells decreases. However, during continued exposure to the acid, the intracellular pH gradually returns to a value near its starting value ($\tau \sim 5$ min). The subsequent removal of the acid triggers a similar transient increase in pH. Results in figure 5 are for just one cell. However, our fluorescence images simultaneously provide estimates of pH in all 50-100 cells in the image. The mean resting pH across cells in this experiment was 6.93 ± 0.16 (n = 88). Adding acid lowered the pH by 0.23 ± 0.04, followed by recovery at an initial rate of 0.04 ± 0.01 pH units/min. Removing the acid caused the pH to rise by 0.42 ± 0.11, then recover at an initial rate of 0.05 ± 0.02 pH units/min.

These results demonstrate that fluorescence microscopy can be used to characterize pH changes in cochlear hair cells of the alligator lizard. We are currently working on experiments to measure changes in flourescence during acoustical stimulation—experiments that will directly assess the effect of acoustic stimulation on the regulation of intracellular pH.

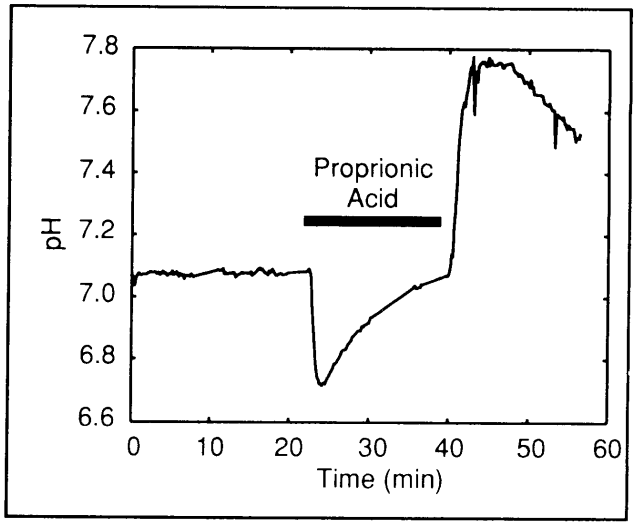

Figure 5. Change in intracellular pH as a function of time during perfusion of proprionic acid. During the first interval of this experiment, the cochlea was bathed in artificial perilymph. During the second interval, which is indicated in this figure by the bar, 20 mM proprionic acid was added to the bath. The perfusate in the third interval was the same as that in the first interval.

1.2.9 Publications

Journal Articles

Duncan, R.K., H.N. Hernandez, and J.C. Saunders. "Relative Stereocilia Motion of Chick Cochlear Hair Cells during High-frequency Water-jet Stimulation." *Aud. Neurosci.* 1: 321-329 (1995).

Shah, D.M., D.M. Freeman, and T.F. Weiss. "The Osmotic Response of the Isolated, Unfixed Mouse Tectorial Membrane to Isosmotic Solutions: Effect of Na^+, K^+, and Ca^{2+} Concentration." *Hear. Res.* 87: 187-207 (1995).

Published Meeting Papers

Davis, C.Q., Z.Z. Karu, and D.M. Freeman. "Equivalence of Block Matching and Optical Flow Based Methods of Estimating Sub-pixel Displacements." *IEEE International Symposium for Computer Vision,* 1995, pp. 7-12.

[14] D. Ronan and E.A. Mroz, "Stability of Solute Composition in a Simple Hair-cell Model," *Abstracts of the Nineteenth Midwinter Research Meeting of the Association for Research in Otolaryngology,* St. Petersburg, Florida, February 4-8, 1996.

Meeting Papers Presented

Davis, C.Q., and D.M. Freeman. "Direct Observations of Sound-induced Motions of the Teticular Lamina, Tectorial Membrane, Hair bundles, and Individual Stereocilia." *Abstracts of the Eighteenth Midwinter Research Meeting of the Association for Research in Otolaryngology,* February 1995, pp. 189.

Freeman, D.M., and T.F. Weiss. "Species Dependence of Osmotic Responses of the Tectorial Membrane: Implications of Structure and Biochemical Composition." *Abstracts of the Eighteenth Midwinter Research Meeting of the Association for Research in Otolaryngology,* February 1995, pp. 188.

Freeman, D.M., and C.Q. Davis. "Using Video Microscopy to Characterize Micromechanics of Biological and Man-made Micromachines." Solid-State Sensor and Actuator Workshop, Hilton Head Island, South Carolina, June 2-6, 1996. Forthcoming.

Shah, D.M., D.M. Freeman, and T.F. Weiss. "The Osmotic Response of the Isolated, Unfixed Mouse Tectorial Membrane: Effect of Na^+, K^+, and Ca^{2+} Concentration." *Abstracts of the Eighteenth Midwinter Research Meeting of the Association for Research in Otolaryngology,* February 1995, pp. 117.

1.3 Auditory Neural Processing of Speech

Sponsor

National Institutes of Health
Grant R01-DC02258
Grant T32-DC00038

Project Staff

Dr. Bertrand Delgutte, Dr. Peter Cariani, Benjamin M. Hammond, Sridhar Kalluri, Martin F. McKinney

The long-term goal of this project is to determine how speech is coded in brainstem auditory nuclei, particularly the inferior colliculus. In the past year, we have written a review of this research area and concentrated on three projects: (1) the neural representation of vowel formants; (2) the neural encoding of amplitude modulations in speech; and (3) functional models of cochlear nucleus neurons for speech processing.

We are continuing a collaborative study of the coding of vowel formants in the auditory nerve with Dr. Tatsuya Hirahara from the NTT Basic Research Laboratories in Tokyo. Formant frequencies are important for vowel perception, yet their neural representation is poorly understood, particularly in the low frequency region where individual harmonics near the formant frequency are psychophysically resolved. Recent psychophysical results of Dr. Hirahara suggest that the phonetic boundary between certain vowels depends on the amplitude ratio of two "crucial" harmonics spanning the first-formant frequency (F1). We are investigating the auditory representation of vowels by recording the activity of auditory-nerve fibers (ANFs) in anesthetized cats in response to /i/-/e/ synthetic-vowel continua. For vowels with high fundamental frequencies (350 Hz), the crucial harmonics were directly represented in ANF responses, whereas the first formant frequency was not. Specifically, profiles of average discharge rate against characteristic frequency (CF) always showed local maxima at the frequencies of crucial harmonics rather than at F1. Furthermore, interspike intervals occurred at the periods of these harmonics rather than at the formant period (1/F1). These findings lend support to the hypothesis put forth by Dr. Hirahara that the fine spectral structure near the first formant is important for vowel perception. This hypothesis is at variance with the widely-held view of vowel perception that vowel identity is based on the spectral envelope derived through wide-band spectral integration. Together, our physiological results and Hirahara's psychophysical findings argue for a new model of vowel perception in which crucial information about fine spectral structure would play a key role.

Speech shows intense vowels alternating with relatively weak consonants. This alternation results in pronounced amplitude modulations near 3-4 kHz that are important for speech understanding. As a first step toward understanding the neural encoding of these modulations, we measured modulation transfer functions (MTFs) and responses to speech utterances in ANFs of anesthetized cats. The ANF-MTF relates (as a function of modulation frequency) the modulation index of an AM stimulus to that of the neural response. ANF-MTFs were bandpass, with high frequency cutoffs in the range 200-700 Hz, reflecting the inability of ANFs to follow fast modulations. Low frequency cutoffs were typically between 3 and 50 Hz, indicating a reduction in the ability to follow slow modulations, consistent with adaptation. A three-stage model incorporating bandpass filtering, instantaneous compression, and the ANF-MTF simulated the envelope of responses to speech utterances. These results indicate that the MTF is useful for predicting neural responses to speech and this concept may also be useful for predicting the responses of central auditory neurons.

They further suggest that improved estimates of speech intelligibility in noise and reverberation might be developed by taking into account the MTFs of auditory neurons.

As a first step towards developing functional models of auditory neurons for speech processing, we are developing a model of onset responders in the cochlear nucleus (CN). These cells, which are characterized by a prominent peak at the onset of the stimulus in their tone-burst evoked peri-stimulus time (PST) histograms, are of particular interest because they respond to acoustic transients that are important in speech perception. Our single-node circuit model of onset cells receives model ANF inputs via excitatory synapses that are implemented by time-varying conductances. Onset PST histograms are obtained in model cells with short membrane time constants and many subthreshold synaptic inputs. By varying the number of model ANF inputs and the strength of these inputs, we can achieve various onset responses such as On-I and On-L as well as primary-like responses. However, the model fails to simulate the physiological observation that off-CF subthreshold tones enhance onset-cell responses to CF tones. This failure may be due to the asynchrony of AN inputs of different CF introduced by the traveling wave along the basilar membrane. We are examining simplified models to better identify the mechanisms that give rise to this cross-frequency summation.

1.3.1 Publications

Journal Articles

Cariani, P.A., and B. Delgutte. "Neural Correlates of the Pitch of Complex Tones. I. Pitch and Pitch Salience." *J. Neurophys.* Forthcoming.

Cariani, P.A., and B. Delgutte. "Neural Correlates of the Pitch of Complex Tones. II. Pitch Shift, Pitch Ambiguity, Phase Invariance, Pitch Circularity, Rate Pitch and the Dominance Region for Pitch." *J. Neurophys.* Forthcoming.

Chapter in a Book

Delgutte, B. "Auditory Neural Processing of Speech." In *Handbook of Phonetic Sciences.* eds. W.J. Hardcastle and J. Laver. Oxford: Blackwell. Forthcoming.

Meeting Papers Presented

Hammond, B.M., and B. Delgutte. "Modulation Transfer Functions of Auditory-nerve Fibers: Measurements and Use in Predicting the Neural Response to Speech." *Abstracts of the Nineteenth Midwinter Research Meeting of the Assocociation for Research in Otolaryngology,* St. Petersburg, Florida, February 4-8, 1996, p. 78.

Hirahara, T., P.A. Cariani, and B. Delgutte. "Representation of Low-frequency Vowel Formants in the Auditory Nerve." *Abstracts of the Nineteenth Midwinter Research Meeting of the Association for Research in Otolaryngology,* St. Petersburg, Florida, February 4-8, 1996, p. 80.

McKinney, M.F., and B. Delgutte. "Physiological Correlates of the Stretched Octave in Interspike Intervals of Auditory-nerve Fibers." *Abstracts of the Eighteenth Midwinter Research Meeting of the Assocociation for Research in Otolaryngology,* St. Petersburg, Florida, February 1995, p. 175.

1.4 Binaural Interactions in Auditory Brainstem Neurons

Sponsor

National Institutes of Health
Grant P01-DC00119

Project Staff

Dr. Bertrand Delgutte, Dr. Ruth Y. Litovsky

The overall goal of this project is to characterize neural mechanisms for sound localization in the auditory midbrain. Studies conducted in the past year were aimed at comparing two possible neural codes for the location of sound sources: an average-rate code, and a temporal code. For this purpose, we made use of an existing data base on responses of inferior-colliculus (IC) neurons to "virtual space" stimuli. In this technique, closed acoustic systems are used mimic the sound pressure waveforms produced in the ear canals of cats by sound sources originating from different directions. The specific stimulus used in these experiments was a 200-msec burst of pseudo-random broadband noise.

The sensitivity index d' was used to characterize the ability of single IC neurons to discriminate sound sources differing in virtual azimuth or elevation. This index makes it possible to compare psychophysical performance with that of an ideal

observer that would optimally process information available in neural responses. The sensitivity index was computed for two response measures: discharge rate averaged over the duration of the stimulus, and a small number (< 6) of principal components that concisely describe the temporal patterns of neural discharge for our stimuli.

For some neurons, d' based on average rates was within a factor of 2-3 of psychophysical performance over a narrow range of azimuths or elevations. Psychophysical performance could be approached over a broader range by selecting for each azimuth of elevation the neuron that gave the best performance. This finding suggests that psychophysical performance in discriminating the position of sound sources can be accounted for by average rate information available in a small fraction of the available pool of IC neurons.

For most neurons, performance based on the principal components was generally better than that based on average discharge rate, particularly when discharge rate showed a plateau as a function of azimuth or elevation. However, this advantage of the temporal code was minimal for the neurons that showed the best performance based on average rate alone. This result suggests that there would be little advantage in using a temporal code over a rate code for the location of sound sources at the level of the IC, except in conditions when average rate information from the most sensitive neurons would be degraded.

1.5 Electrical Stimulation of the Auditory Nerve

Sponsor

National Institutes of Health
Grant P01-DC00361

Project Staff

Dr. Bertrand Delgutte, Scott B.C. Dynes

The overall goal of this project is to study the physiological mechanisms of electrical stimulation of the cochlea to help design better processing schemes for cochlear implants. Experiments conducted last year were aimed at characterizing auditory-fiber correlates of interactions observed psychophysically when pulsatile electric stimuli are applied in rapid succession. Such interactions are likely to play an important role in the popular continuous interleaved sampling (CIS) speech processors. We are also evaluating Hodgkin-Huxley-like models of nerve membrane for the stimuli used in our experiments.

In our experiments conducted in anesthetized cats, a conditioner consisting of one or more pulses of equal amplitude, is used to modify the state of an auditory-nerve fiber. This conditioner is followed at various delays by a single pulse used to probe the state of the modified fiber. The neural threshold and dynamic range are measured for the probe pulse following various conditioners. Subthreshold conditioners result in a short period (< 1 msec) of sensitization, followed by a longer (4-5 msec) desensitization period. Sensitization decreases with increasing numbers of conditioning pulses. The neural dynamic range is increased during the sensitization period. Suprathreshold conditioners lead to a relative refractory period, with probe threshold resuming its resting value after 4 msec. There was no significant change in the relative refractory period as the number of pulses and interpulse intervals were varied. Following a suprathreshold conditioner, the dynamic range is decreased for short probe delays.

Modeling studies show that these experimental phenomena can be qualitatively reproduced using standard Hodgkin-Huxley-like models. Specifically, the Hodgkin-Huxley model of the squid giant axon and the Rothman-Manis-Young model of cochlear nucleus bushy cells provided simulations that were broadly consistent with the data. In contrast, models of mammalian systems (rat and rabbit sciatic nerve) provided poor simulations of the data, apparently because the time constants of their state variables are much quicker than those controlling cat auditory nerve fibers. A stochastic extension of the Hodgkin-Huxley model was developed in order to simulate the probabilistic character of neural responses. There was qualitative agreement between this stochastic model and the experimental data on how the dynamic range is affected by conditioning pulses.

It is clear that the type of temporal interactions we have studied must occur for present-day cochlear implant stimulation strategies. For a typical CIS processor, the interpulse interval for individual electrodes is less than 1 msec. The temporal interactions seen experimentally with sub- and suprathreshold conditioners last much longer, typically 4-5 msec. Moreover, the magnitude of the sensitization and desensitization due to temporal interactions are a significant fraction of the 12 dB perceptual dynamic range of human cochlear implant subjects.

Our finding that Hodgkin-Huxley-like models can simulate most of the experimental results suggests that the same models might be used to predict responses to the more complex stimuli produced by CIS processors. If so, it might be possible to use these models to determine the electrical stimulus

needed to produce a desired pattern of activity in the auditory nerve, and thereby help design improved processing schemes.

1.5.1 Publications

Meeting Papers Presented

Delgutte, B., and S.B.C. Dynes. "Implications of Auditory Neural Coding for Signal Processing in Cochlear Implants." Abstracts of the 1995 Conference on Implantable Auditory Prostheses, Asilomar, California, p. 1, 1995.

Dynes, S.B.C., and B. Delgutte. "Temporal Interactions of Electric Pulses in the Auditory Nerve: Experiments and Modeling." Abstracts of the 1995 Conference on Implantable Auditory Prostheses, Asilomar, California, p. 43, 1995.

Thesis

Dynes, S.B.C. *Discharge Characteristics of Auditory-nerve Fibers for Pulsatile Electrical Stimuli.* Ph.D. diss. Dept. of Physics, MIT, 1995.

1.6 Cochlear Efferent System

Sponsor

National Institutes of Health
Grant 2RO1 DC00235

Project Staff

Dr. John. J. Guinan, Jr., Christopher A. Shera, Konstantina M. Stankovic

Our aim is to understand the physiological effects produced by efferents in the mammalian inner ear including medial olivocochlear efferents, which terminate on outer hair cells, and lateral efferents, which terminate on auditory-nerve fibers.

During the past year, we have continued publishing our work on a class of vestibular primary afferent neurons that arise in the saccule and respond to sound at moderately high sound levels. A previously submitted paper was revised and published.[15] A paper that summarized our results and pointed out that certain acoustically-evoked neck-muscle reflexes appear to be mediated by these acoustically responsive vestibular fibers was submitted for publication.[16]

In a recently submitted manuscript,[17] we show that efferent inhibition of auditory-nerve fibers is largest at moderate to high sound levels, a finding that is unexpected with most current theories of the action of efferents. Previous work has shown that medial efferents can inhibit responses of auditory-nerve fibers to high-level sounds and that fibers with low spontaneous rates (SRs) are inhibited most. However, quantitative interpretation of these data was made difficult by effects of adaptation. To minimize systematic differences in adaptation, we measured efferent inhibition with a randomized presentation of both sound level and efferent stimulation. In anesthetized cats, we stimulated efferents with 200/s shocks and recorded auditory-nerve-fiber responses to tone bursts (0-100 dB SPL, 5 dB steps) at their characteristic frequencies. Below 50 dB SPL, efferent inhibition (measured as equivalent attenuation) was similar for all fibers with similar CFs in the same cat. At 45-75 dB SPL, low-SR and medium-SR fibers often showed inhibition that was much larger than at low sound levels. At 90-100 dB SPL, these fibers still had substantial inhibition even. Expressed as a fractional decrease in rate, at 90-100 dB SPL the inhibition was 0 percent, 6 percent and 13 percent for high-, medium- and low-SR fibers with the differences statistically significant. Finding the largest equivalent attenuations at 45-75 dB SPL does not fit with the hypothesis that medial-efferent inhibition is due solely to a reduction of basilar-membrane motion. The large attenuations, some over 50 dB, indicate that medial efferent inhibition is more potent than previously reported. During the past year we pre-

---

[15] M.P. McCue and J.J. Guinan, Jr., "Spontaneous Activity and Frequency Selectivity of Acoustically Responsive Vestibular Afferents in the Cat," *J. Neurophys.* 74: 1563-1572 (1995).

[16] M.P. McCue and J.J. Guinan, Jr. "Sound-Evoked Activity in Primary Afferent Neurons of the Mammalian Vestibular System," submitted to *Am. J. Otology.*

[17] J.J. Guinan, Jr., and K.M. Stankovic, "Medial Efferent Inhibition Produces the Largest Equivalent Attenuations at Moderate to High Sound Levels in Cat Auditory-nerve Fibers," submitted to *J. Acoust. Soc. Am.*

sented this work along with work comparing the time course of efferent effects.[18]

In work done with M.C. Liberman and S. Puria,[19] we developed a method for measuring ipsilaterally-evoked efferent inhibition by measuring the time course of its effect on distortion-product otoacoustic emissions (DPOAEs). In anesthetized cats, the onset behavior of the DPOAE at 2f1-f2 produced by primary tones at frequencies f1 and f2 (f1<f2) was measured with temporal resolution finer than 70 msec. After the onset of the primary tones, the DPOAE adapted by as much as 6 dB for monaural stimulation and 10 dB when the primaries were presented binaurally. DPOAE adaptation consisted of a large, rapid component (time constant approximately 100 msec), and a small, slower component (time constant approximately 1000 msec). The rapid component disappeared when the olivocochlear bundle (OCB) was cut, whereas the slow adaptation persisted. The loss of rapid adaptation after OCB section was accompanied by a concomitant increase in the steady-state amplitude of the DPOAE. Thus, an intact OC reflex can significantly depress DPOAEs during routine measurements. Tests for the ipsilateral OC reflex based on the phenomenon of rapid adaptation should be both feasible and useful in human subjects. Also during the past year, a previously submitted paper has been revised and accepted.[20]

Also during the past year, a chapter on "The Physiology of Olivocochlear Efferents" was submitted and accepted.[21]

1.6.1 Publicatons

Journal Articles

Guinan, J.J., Jr., and K.M. Stankovic. "Medial Efferent Inhibition Produces the Largest Equivalent Attenuations at Moderate to High Sound Levels in Cat Auditory-nerve Fibers." *J. Acoust. Soc. Am.* Forthcoming.

Liberman, M.C., S. Puria, and J.J. Guinan, Jr. "The Ipsilaterally Evoked Olivocochlear Reflex Causes Rapid Adaptation of the 2f1-f2 DPOAE." Submitted to *J. Acoust. Soc. Am.*

McCue, M.P., and J.J. Guinan, Jr. "Spontaneous Activity and Frequency Selectivity of Acoustically Responsive Vestibular Afferents in the Cat." *J. Neurophys.* 74: 1563-1572 (1995).

McCue, M.P., and J.J. Guinan, Jr. "Sound-Evoked Activity in Primary Afferent Neurons of the Mammalian Vestibular System. Submitted to *Am. J. Otology.*

Puria, S., J.J. Guinan, Jr., and M.C. Liberman. "Olivocochlear Reflex Assays: Effects of Contralateral Sound on Compound Action Potentials vs. Ear-canal Distortion Products." *J. Acoust. Soc. Am.* 99: 500-507 (1996).

Chapter in a Book

Guinan, J.J., Jr. "The Physiology of Olivocochlear Efferents." In *The Cochlea.* Eds. P.J. Dallos, A.N. Popper, and R.R. Fay. New York: Springer-Verlag. Forthcoming.

Meeting Paper Presented

Guinan, J.J., Jr., and K.M. Stankovic. "Medial Olivocochlear Efferent Inhibition of Auditory-nerve Firing Mediated by Changes in Endocochlear Potential." *Abstracts of the Eighteenth Midwinter Research Meeting of the Association for Research in Otolaryngology,* February 1995, p. 172.

---

[18] J.J. Guinan, Jr., and K.M. Stankovic, "Medial Olivocochlear Efferent Inhibition of Auditory-nerve Firing Mediated by Changes in Endocochlear Potential," *Abstracts of the Eighteenth Midwinter Meeting of the Association for Research in Otolarngology,* St. Petersburg, Florida, February 1995, p. 172.

[19] M.C. Liberman, S. Puria, and J.J. Guinan, Jr., "The Ipsilaterally Evoked Olivocochlear Reflex Causes Rapid Adaptation of the 2f1-f2 DPOAE," submitted to *J. Acoust. Soc. Am.*

[20] S. Puria, J.J. Guinan, Jr., and M.C. Liberman. "Olivocochlear Reflex Assays: Effects of Contralateral Sound on Compound Action Potentials vs. Ear-canal Distortion Products," *J. Acoust. Soc. Am.* 99: 500-507 (1996).

[21] J.J. Guinan, Jr., "The Physiology of Olivocochlear Efferents," in *The Cochlea,* eds. P.J. Dallos, A.N. Popper, and R.R. Fay (New York: Springer-Verlag, forthcoming).

1.7 Interactions of Middle-Ear Muscles and Olivocochlear Efferents.

Sponsor

National Institutes of Health
Grant P01 DC00119

Project Staff

Dr. John J. Guinan, Jr.

Our aim is to determine the actions and interactions of the acoustically elicited middle-ear muscle reflexes and the olivocochlear efferent reflexes.

During the reporting period, we have begun a project aimed at determining the pathways of the medial olivocochlear efferents. For three reflexes which affect transmission of signals through the peripheral auditory system: the stapedius muscle, the tensor-tympani muscle, and the medial olivocochlear efferents, we know the locations of the effector neurons but not the locations of the brainstem interneurons neurons which relay information from the auditory nerve to the motoneurons. By selectively lesioning various areas in the cochlear nucleus with injections of kainic acid and monitoring the resulting changes in these reflexes, we hope to determine which areas of the cochlear nucleus contain interneurons which mediate these reflexes. Initial work shows that with kainic acid injections that destroy or damage substantial parts of the cochlear nucleus, the medial olivocochlear efferent acoustic reflex remains intact.

1.8 Cochlear Implants

Sponsor

National Institutes of Health
Grant P01-DC00361
Contract N01-DC22402

Project Staff

Dr. Donald K. Eddington, Dr. Robert D. Hall, Arash Lighvani, Christopher McKinney

The basic function of a cochlear prosthesis is to provide a measure of hearing to the deaf by using stimulating electrodes implanted in or around the cochlea to elicit patterns of spike activity on the array of surviving auditory-nerve fibers. By modulating the patterns of neural activity, these devices attempt to present information that the patient with the implant can learn to interpret. The spike activity patterns elicited by electrical stimulation depend on several factors: the complex, electrically heterogeneous structure of the cochlea, the geometry and placement of the stimulating electrodes, the stimulus waveform, and the distribution of surviving nerve fibers. An understanding of how these factors interact to determine the activity patterns is fundamental to designing better devices and interpreting the results of experiments involving intracochlear stimulation of animal and human subjects.

As a first step toward achieving this understanding, we are developing a software model of the cochlea that predicts the distribution of potential produced by stimulation of arbitrarily placed, intracochlear electrodes. These potential distributions will be used as inputs that drive models of auditory-nerve fibers to compute neural activity patterns produced by intracochlear stimulation.

The initial model reported in previous *RLE Progress Reports* was formulated by digitizing sections of a human temporal bone with each spatial sample representing a specific tissue or fluid (e.g., bone, nerve, perilymph, membrane). Based on the material represented, each sample was assigned a resistivity and a finite difference technique was used to convert these data to a set of equations designed to represent the nonhomogeneous electrical structure of the cochlea. Current sources were added to the model at nodes representing the positions of the six intracochlear electrodes implanted in a number of deaf human subjects at the Massachusetts Eye and Ear Infirmary.

The human model has been tested by comparing the model predictions of intracochlear potential distributions computed for stimulation through a single electrode with intracochlear potentials measured at five unstimulated electrodes in human subjects when a sixth was stimulated. Model results predicted the asymmetric and, for some stimulation sites, nonmonotonically decreasing potentials measured in the human subjects.

While these initial tests are encouraging, the human model does not lend itself to comprehensive testing because of the restrictions placed on the location of electrodes and on the anatomical manipulations appropriate in human subjects. In order to provide wider latitude in testing, a similar model was implemented for the rat where the experimental subject can be sacrificed and the temporal bones quickly prepared for anatomical analysis.

The rat model is based on 105 histological sections, every fifth section of a series cut 5 μm thick and registered using 200-μm holes drilled in the embedded cochlea before sectioning. Outlines of cochlear structures were drawn on digital images using Image software with a resolution of 6.25 μm. Twenty-two different tissues or fluids were assigned

unique tags that could be converted to a specific resistance when the model was implemented.

Tests of the model were made in the rat by measuring the potential at four unstimulated electrodes when current was injected monopolarly (ipsilateral pinna reference) through a fifth and comparing the potentials with corresponding values predicted by the model. Stimuli were 10-μÅ sinusoidal pips. Potentials recorded between the intracochlear electrodes and the contralateral ear were averaged and measured peak-to-peak.

The five intracochlear Pt-Ir electrodes, implanted through holes in the capsule or through the round window, had cylindrical tips 100 μm-long. Their locations were determined in histological sections. Electrode implantation and all measurements were made in deeply anesthetized animals.

Figure 6 shows data from a single animal to illustrate three consistent features of the potentials recorded from 10 animals: (1) stimulation at apical sites produced large potentials with steep gradients; (2) stimulation at basal sites resulted in somewhat smaller potentials with flatter gradients; and (3) stimulus frequency, from 100 Hz to 10 kHz, had no significant effect on the amplitude of the recorded potentials, consistent with the assumption of no large capacitive effects of the tissues.

Histological evaluation of the cochleas revealed significant disturbance of tissues in the immediate vicinity of some electrodes (longitudinal extent less than 0.5 mm in most cases), indicating that predictions by the "normal" model might not be appropriate. The model was therefore modified to reflect abnormalities such as spiral ligament displacement and rupture of the basilar membrane.

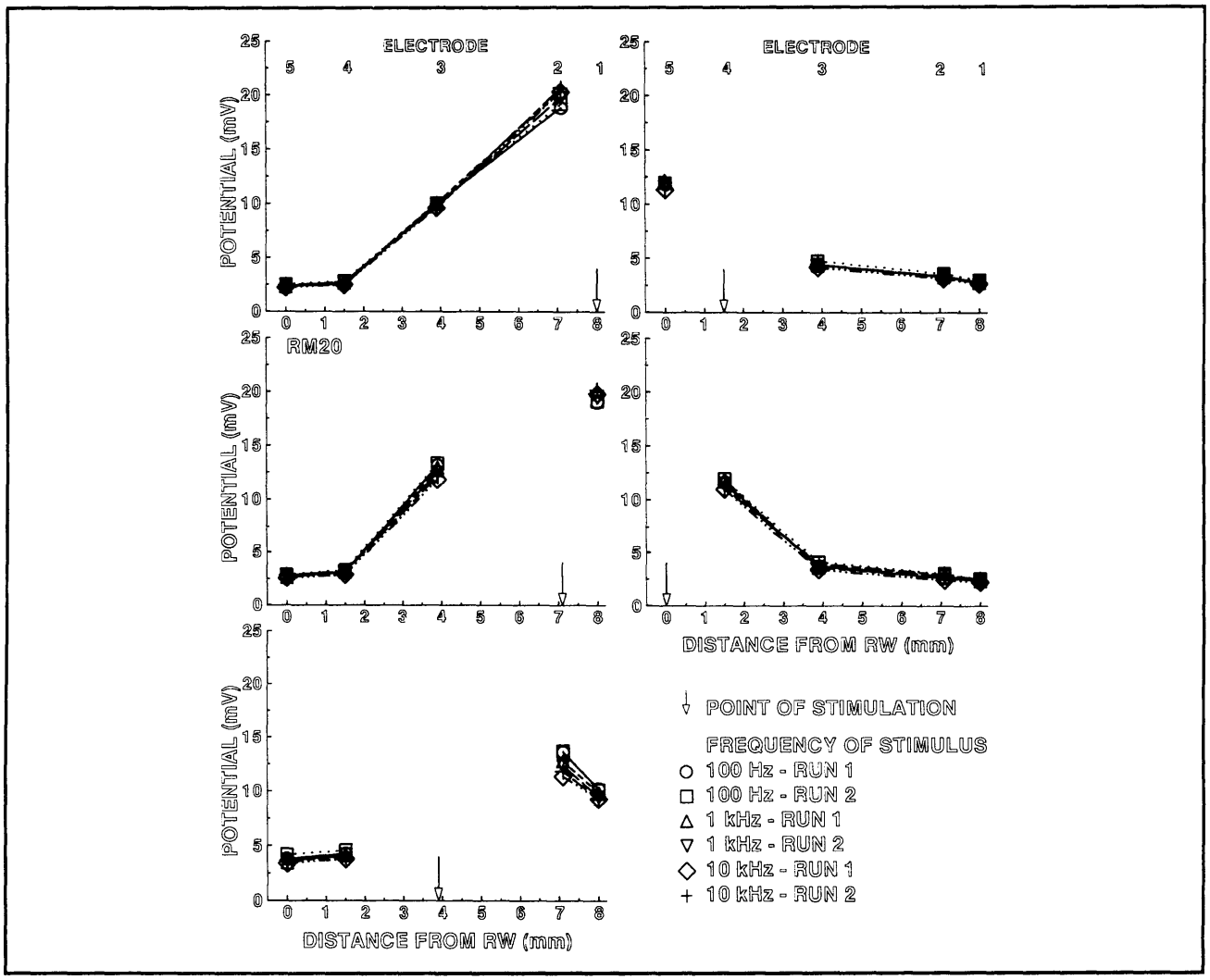

Figure 6. Cochlear potential measured at unstimulated, intracochlear electrodes (symbols) as a function of electrode position. The arrow in each panel shows the position of the stimulating electrode. The frequency of the sinusoidal stimuli are keyed by symbol.

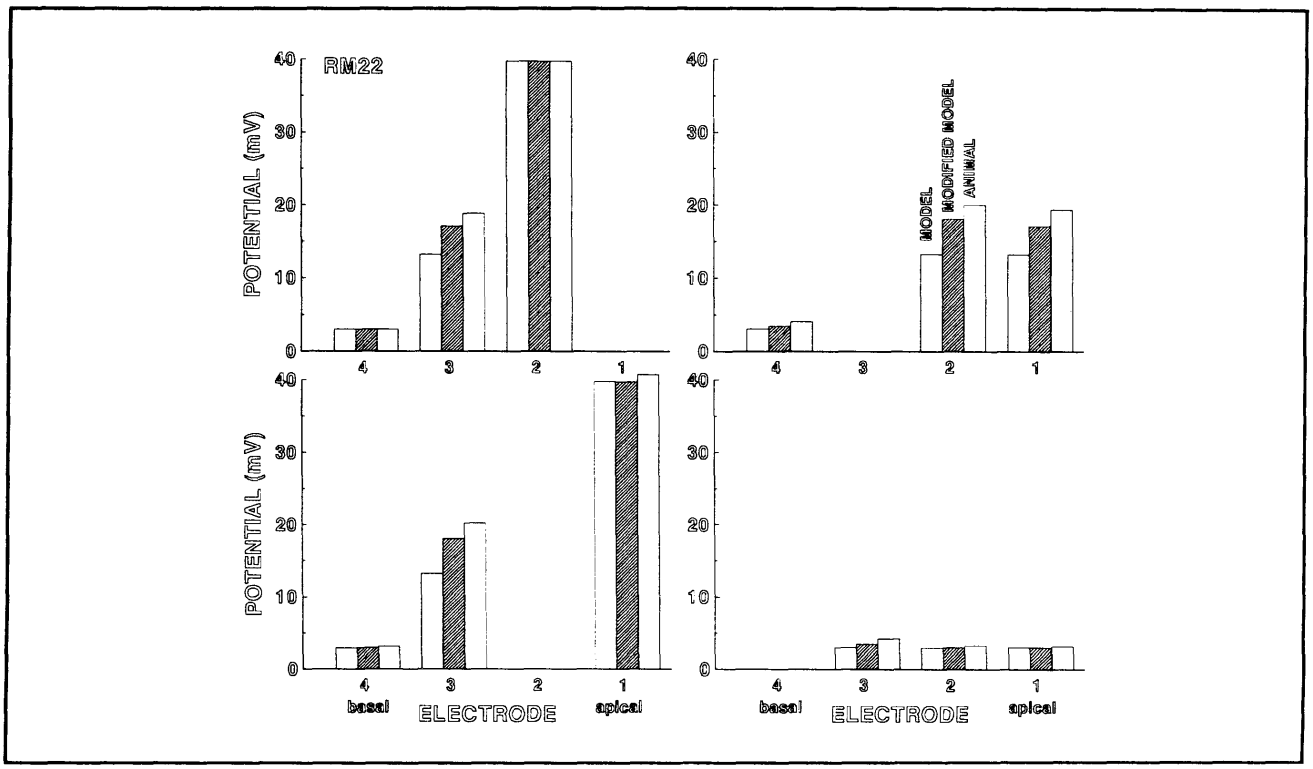

Figure 7. Normalized potentials measured at the unstimulated, intracochlear electrodes in a single rat and normalized potential predictions computed by the "normal" model and a model "modified" to represent the details of the animal's cochlear pathology. Data are not presented for electrode five because it was positioned outside the cochlea in this animal.

Figure 7 illustrates the general result that the potentials predicted by the "normal" and "modified" models for each rat did not differ by very much at the locations of the unstimulated electrodes. Where they were appreciably different, predictions of the modified model were nearly always closer to the potentials measured in the animals than were those of the normal model.

The modifications in the model did have a relatively large effect on the potential distributions, but were confined to the tissues and fluids in the immediate region of the stimulating electrode. This can be seen in figure 8, where scala media potentials predicted by the normal and modified models are plotted. Scala media potentials were selected for this illustration because they represent the largest differences between the two models for this animal.

These initial results indicate that this electro-anatomical model of the rat's cochlea predicts with fairly good accuracy the potentials measured at unstimulated electrode sites. Manipulations of the model structure to more accurately reflect the cochlear pathology induced by the placement of intracochlear electrodes in five rat subjects led to significant improvements of the model predictions in most cases. In the next series of animal tests, we plan to measure potentials close to the stimulating electrode where (1) the potentials are relatively high, (2) the gradients are relatively steep, and (3) the model predicts the largest effects of cochlear pathology.

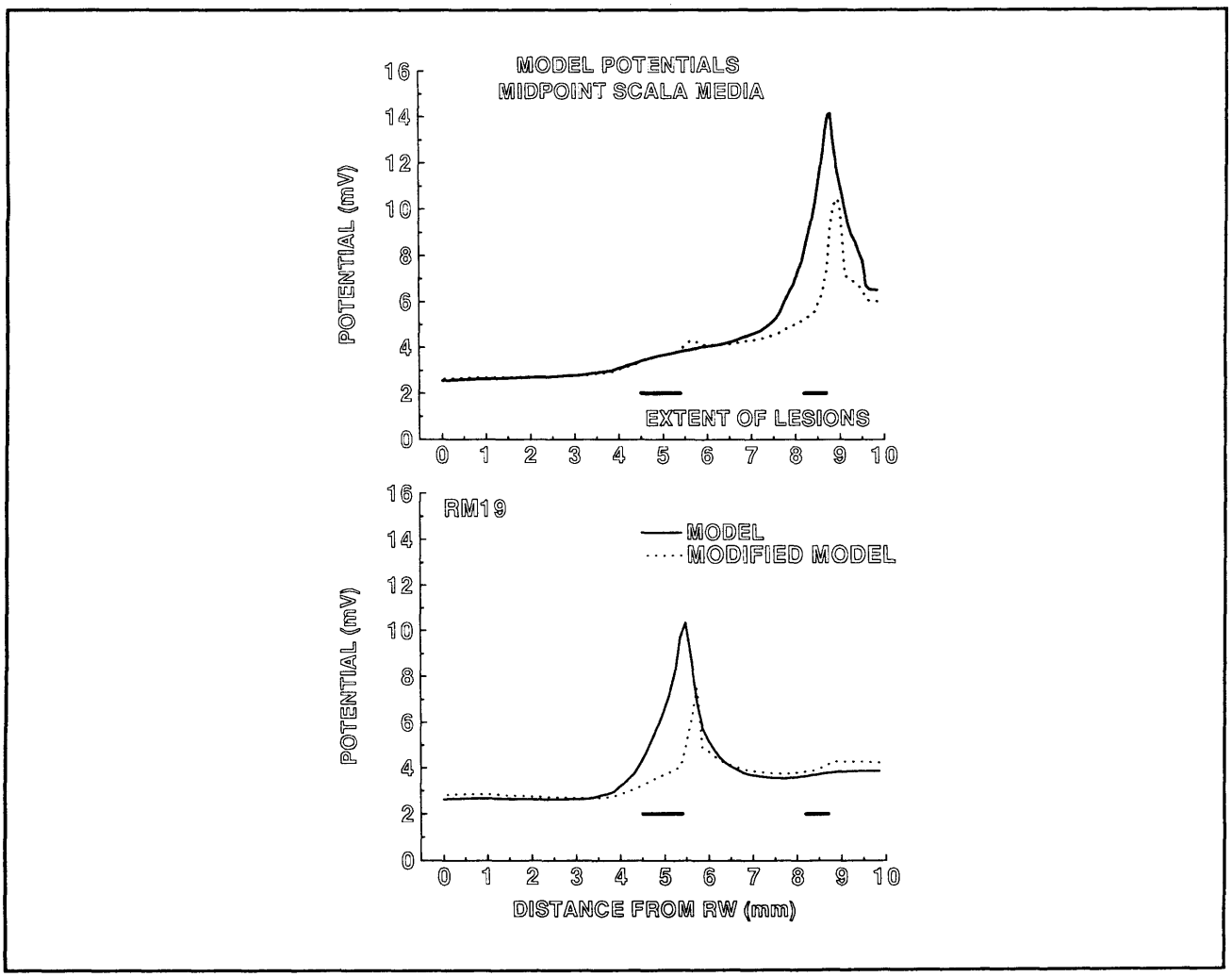

Figure 8. Scala media potentials predicted for the "normal" and "modified" models. Modifications of the model were made for sections included within the extent of the lesions as indicated.